Electronic Supplementary Material (ESI) for Physical Chemistry Chemical Physics.

Supporting Informations

Water transport within carbon nanotubes on a wave

Jin-Yi Li, Zeng-Qiang Wu, Jing-Juan Xu*, Hong-Yuan Chen, Xing-Hua Xia*

State Key Laboratory of Analytical Chemistry for Life Science and Collaborative Innovation Center of Chemistry for Life Sciences, School of Chemistry and Chemical Engineering, Nanjing University, Nanjing, 210023, China

Corresponding Author E-mail: xhxia@nju.edu.cn, xujj@nju.edu.cn

I. CNT construction with different types

A graphene sheet is first set up by importing the coordinates with all carbon atoms. We choose the under-rolling direction according to the value of *m* and *n* in CNTs. The under-rolling direction is set as X-axis. The direction (Y-axis) perpendicular to the X-axis is then calculated (5,-7) and noted as the axial direction of CNTs. All the concerning carbon atoms (within the red rectangle in **Fig. 3a**) are rolled up by transformation of coordinates with equation S1:

$$\begin{cases} x' = R_{CNT}\cos\left(\dfrac{x}{R_{CNT}}\right) \\ y' = R_{CNT}\sin\left(\dfrac{x}{R_{CNT}}\right) \\ z' = y \end{cases} \tag{S1-1}$$

$$R_{CNT} = \frac{\sqrt{3}B_{cc}}{2\pi}\sqrt{m^2+mn+n^2} \tag{S1-2}$$

where, B_{cc}=1.42 Å is the average carbon-carbon bond length in CNTs. *x*, *y*; *x*', *y*' and *z*' are the coordinates of graphene and CNT, respectively. Since the *m* and *n* are both integers, the radii of CNT are discrete numbers.

II. Three approximations in treating CNTs as a uniformly cylindrical tube

We treat the van der Waals (vdW) force of carbon in CNTs and water as L-J potential. The equation writes:

$$U_{LJ}\left(r_{ij}\right) = \varepsilon_{ij}\left[\left(\frac{R_{\min,ij}}{r_{ij}}\right)^{12} - 2\left(\frac{R_{\min,ij}}{r_{ij}}\right)^{6}\right] \tag{S2-1}$$

where

$$\varepsilon_{ij} = \sqrt{\varepsilon_i \varepsilon_j} \tag{S2-2}$$

where, $R_{min,ij}$ is the minimum-potential distance of atom *i*, *j* and defined as $R_{\min,ij}=(R_{\min,i}+R_{\min,j})/2$, while $R_{min,i}$ and $R_{min,j}$ are parameters referring from CHARMM force field. (**Table S1**)

When $r_{ij}=R_{\min,ij}$, equation (S2-1) gains the minimum potential because the first derivative of the equation equals to zero. Considering $R_{\min,CO}$-$R_{\min,CH}$=1.543>B_{OH}=0.9572, which means the vdW force of CNTs wall and hydrogen in water can be neglected.

Another approximation comes from neglecting the chirality of CNTs. When water molecule is situated at the optimum position (*i.e.* the lowest vdW interactions) within CNTs, the variation of vdW force between water and the wall by different arrangements can also be neglected. **Fig. S1a-b** shows the vdW potential of a single oxygen (or water, which is proved in the above paragraph) at different positions.

When water molecule deviates from the optimum position and becomes closer to the

wall, the fluctuation of potential occurs. The corrugated "mouth of glass" in **Fig. S1a** shows the fluctuation. **Fig. S1b** represents the L-J potential of y=0 (red frame in **Fig. S1a**). At the optimum position, the fluctuation is less than 1 cal/mol (**Fig. S1c-d**). As a contrast, the average velocity of water in CNTs is about 500 m/s (**Fig. S1e**); therefore, the kinetic energy is about 536 kcal/mol and 5 orders of magnitude larger than fluctuation. Consequently, we ignore the fluctuation and consider that the water transport will not be affected by the chirality of CNTs.

The third approximation aims at the charge of CNT. Keblinski [1] reported the charge distribution of CNTs (5,5) of length 12 Å. They have shown the atoms with -0.06 e at the mouth of CNTs and the others <0.03e by *ab initio* calculations. In our system, carbons in CNTs are zero-charged for simplicity.

As a result, CNT is then considered as a uniformly cylindrical tube by the above discussions, namely, different arrangements of carbon in CNTs with the same radius are undistinguishable.

Furthermore, as radius of CNT (m,n) can be calculated as: R_{CNT}=0.39143$(m^2+n^2+mn)^{1/2}$ Å, the radii of CNT (10,6) and (14,0) are strictly equal, *i.e.*, 5.480 Å. We compare the concerning parameters in **Table S2** and the deviation is less than 5 %.

III. MD simulation details.

The CNT (length: 40 Å) is set along z-axis, while the center of CNT locates at the original point. Two graphene sheets (43 Å × 42 Å) with holes exactly fitting the diameter of CNT are fixed at both mouths of CNT. The outsides of both sheets are water reservoirs. Water molecules are randomly filled in both reservoirs and CNT. Two movable graphene sheets of 680 carbon atoms (without holes, the same size as the ones with holes) are set at the boundaries of both reservoirs. A relatively large force of 0.2 kcal·mol^{-1}·Å^{-1} is exerted on each atom of the movable sheet at –z along the positive direction of Z-axis; and a force of -0.01 cal·mol^{-1}·Å^{-1} is exerted on each atom of the movable sheet at +z to prevent water escape. To evaluate the external pressure, we select a typical radius value of 5.089 Å (CNT type (13,0)) to investigate the influence of pressure on the moving graphene sheets. As shown in **Fig. S2**, the velocity of water at CNT mouth shows linearity with the pressure. However, as the density of water decreases with lower pressure, the ratio of velocity to pressure shows an insignificant increase. As a result, we select the pressure of 1.41 GPa to reduce the cost of simulation.

The simulations are run by NAMD (Nanoscale Molecular Dynamics) [2] with visual software VMD (Visual Molecular Dynamics). [3] The force field used for the simulations is CHARMM (Chemistry at Harvard Molecular Mechanics). [4] Lennard-Jones (L-J) 12-6 Potential describes the vdW interactions, and PME (Particle Mesh Ewald) method [5] is used to calculate the electrostatic interactions. The system temperature is controlled by Langevin dynamics at 300K after minimization. TIP3P (transferable intermolecular potential three-point) water model [6] is to describe water molecules in our system. The parameters for vdW potential are listed in **Table S1**, and the cut-off radius and switching function radius are 10 Å and 9 Å, respectively.

The system executes a geometric minimization process with all graphene sheets fixed. Thus, the equilibrium process takes 1 ns to reach 300K with time-step of 0.5 fs. The external force is applied on both moveable graphene sheets for 1 ns with time-step 1 fs and trajectory time-step of 0.5 ps. In addition, we run short time of 20 ps and 200 ps with trajectory time-step of 1 fs and 10 fs for calculating the vibration of water molecules in CNTs.

Besides, a water box (18 Å×18 Å×40 Å) containing 3636 randomly posited TIP3P water molecules is built for obtaining several parameters such as distances between neighboring waters and average hydrogen bonds per water molecule. A minimization of geometric energy is held before 1 ns equilibrium (time step 0.5 fs). The Langevin dynamics is set up to maintain a steady temperature and pressure. Other parameters are identical to the ones in the above described model. The last 80 % of the trajectory data are used to reduce the instability.

IV. Algorithm of Spheres packing in cylinder

We start our algorithm with the following rules. The cylinder with fixed radius which equals to the radius of CNTs subtracting the vdW radius of carbon in CNTs is obtained. A quantity of sphere seeds with random start coordinates is placed into the cylinder. The sphere seeds represents a sphere with the radius 0 and will become larger during the processes. The radii are enlarged simultaneously if no overlap volume (V_O) existed between sphere and sphere or between sphere and cylinder. The coordinates of spheres will be changed to reduce V_O once V_O is larger than zero. The adjustment of coordinates is a quasi-physical algorithm: Considering that the spheres have elastic potential energies, the deformation caused by overlap results in a pair of forces applying on both spheres. After traversing all the spheres, the vector sum of forces on a single sphere drive the sphere moving along the direction of the vector sum for a fixed time t_0. The adjustment will proceed several times, and has to be interrupted if V_O cannot reduce to V_{lb} (here, V_{lb} represents the lower bound of overlap volume) after the maximum adjusting times $N_{max,A}$ (herein, we set it as a constant: 100). After the loop ends, the radius is raised if V_O reduces to zero (or lower than V_{lb}); the radius is reduced if the loop exceeds $N_{max,A}$ and the increment of radius decreases. When the variation of radius is smaller than r_{lb} (lower bound of radius increment, which can be set as 1×10^{-4}, *etc*, as the accuracy required), the obtained result is the largest radius that the cylinder is able to contain with a fixed number of spheres.

The above algorithm can be improved by adding repacking processes as quite a bit of conditions is stuck, *i.e.*, all spheres are force-balanced but the solution is not the best. When V_O is still greater than V_{lb} after adjustment of coordinates, a random shift with different direction and distance is applied on each sphere. The maximum distance of the shift is not exceeding $R_s/3$ where R_s represents the radius of spheres. After repacking processes, another adjustment of coordinates executes. If the radius is not enlarged during several times of repacking processes, we set the final result as the value of radius. The related content is reconstructed in **Fig. 2**, showing the flow diagram of the processes.

V. Introduction of the packing problem

The packing problem is an optimal strategy to pack objects together into containers. The number of objects is discrete comparing with the size of container, *i.e.*, a 3-meter-circle can hold seven 1-meter circles but a 2.99-meter-circle can only hold five 1-meter circles, [7] demonstrating that the number of small circles is discrete comparing with the radius of large circle. The packing problem is of significance in many fields such as loading and layout designing. In chemistry, it has been utilized in gas sorption and desorption prediction, [8] protein, [9] polydisperse particles [10] and other granular [11] packing. As it is an NP-hard (Non-deterministic Polynomial-time hard) problem, [12] its analytical solution is only available for small systems, and approximate algorithms are essential for relatively large systems. [13]

VI. Sphere radius selection in Packing Problem

As shown in **Fig. S3b**, we replace water molecule into a sphere with the diameter equals to the neighboring oxygen-oxygen-distance (r_{OO}). This replacement is performed according to the following reasons: First, the L-J parameter $R_{min,OO}$ shows that the balanced distance of neighboring oxygen is 3.38 Å, and it will be reduced to r_{OO} (2.72 Å) due to the hydrogen bond. This means that other oxygen can reach the distance of 2.72 Å along the direction of hydrogen bonds, and larger distance up to 3.38 Å for other directions. Therefore, the room of the sphere is forbidden for other water molecules. Second, the radius of the sphere is set as a constant because the pair distribution function (PDF) peak of oxygen atoms is sharp (width at half height: 0.26 Å) and about 1/10 comparing to the peak value (2.72 Å, shown in **Fig. S3c**), where definition of PDF is shown below:

The PDF for oxygen atoms is calculated as: all oxygen atoms are traversed to calculate the distances with other oxygen atoms, and then we obtain the function of the number of distances between r and $r+\Delta r$ with the independent variable r, where r is a given distance. Each oxygen-oxygen-pair is counted twice, which is needed to be halved. The function is divided by $4\pi r^2$ and normalized to achieve PDF.

VII. Definitions and calculations

Effective radius of CNTs: As CNTs can be considered as a uniformed cylindrical tube, we can calculate the L-J interaction between a single water molecule and a CNT with infinity length. Considering CNTs as continuous, the potential of oxygen in single water molecule (hydrogen can be neglected) at the point with the distance a from the origin at the same height (z axis) in CNTs (**Fig. S3a**) is written as:

$$U_{LJ}(a)=\int_{-\infty}^{+\infty}\int_{0}^{2\pi}U(\theta,z)\cos\theta\, d\theta dz \tag{S3-1}$$

therein,

$$U(\theta,z)=\frac{\varepsilon_{CO}r(\theta,z)}{A}\left[\left(R_{\min,CO}/r(\theta,z)\right)^{12}-2\left(R_{\min,CO}/r(\theta,z)\right)^{6}\right] \tag{S3-2}$$

$$r(\theta,z)=\sqrt{\left(-a\cos\theta+\sqrt{R_{CNT}^2-a^2\sin^2\theta}\right)^2+z^2} \tag{S3-3}$$

$$A=\frac{3\sqrt{3}}{4}r_{CC}^2 \tag{S3-4}$$

As shown in **Fig. S3a**, T is the test point, and a is a given distance of point T from origin O. $U_{LJ}(a)$ is the total potential at point T, and $U(\theta,z)$ refers to the contribution of potential at angle of θ and coordination of z; R_{CNT} is the radius of CNTs, while θ and z are the angle and height of integrate unit $\mathrm{d}\theta\mathrm{d}z$; $r(\theta,z)$ is the distance between the integrate unit and point T. A is the average area of a single carbon on the surface of nanotubes. r_{CC} is the bond length of carbon in CNT and a value of 1.42 Å is adopted in calculations referring to CHARMM force field.

After numerical calculating U_{LJ} with different radius as function of a, we define the effective radius r_{eff} at which the presence probability of water molecules is 1 % comparing with the maximum probability, and it is figured out by the following equation and listed in **Table 1** in main body.

$$e^{-\frac{U_{LJ}(r_{eff})}{N_AkT}}=0.01e^{-\frac{U_{LJ}^*}{N_AkT}},\ \text{i.e.,}\ U_{LJ}(r_{eff})=2.75+U_{LJ}^* \tag{S4}$$

where, N_A, k and T refer to the Avogadro constant, the Boltzmann constant and temperature, respectively. U^*_{LJ} is the minimum value of $U_{LJ}(a)$.

distribution function peak of water molecules: The radial distribution function (RDF) peak of water molecules in CNTs (r_{dfp}) is calculated. The number of water molecules (N) with their coordinates reaching $r\leq(x^2+y^2)^{1/2}\leq r+\Delta r$ is first counted, and described as a function of r. The number density (ρ) distribution can then be written:

$$\rho(r)=\frac{N(r)}{\Delta V\cdot Fr}=\frac{N(r)}{2\pi dh\Delta r\cdot Fr} \tag{S5}$$

where, V and r are the volume and the distance from the original point, respectively; h is the length of CNT; Fr is the frame number of trajectory. After a two-peak Gaussian fitting (or single-peak fitting) of the function $\rho(r)$ (Equation S5), the larger peak radius is defined as r_{dfp}. The detailed data are presented in **Table S3**.

Average velocity of water molecules in CNTs: The average velocity of water in CNTs is calculated as follows: The average Z-coordinate value of both movable graphene sheets is calculated for every frame of trajectories, respectively. The velocity of these sheets is determined with a least squares fitting. In consideration of the constancy of water density, the product of flow cross-section of CNTs and the velocity of water molecules in CNTs is equal to the product of sheet area and the velocity of sheets. The velocity of water molecules in CNTs is written as:

$$v_{sheet}=\frac{6\sum_i\left[i\left(Z_{driving,i}+Z_{driven,i}\right)\right]-3(Fr+1)\sum_i\left(Z_{driving,i}+Z_{driven,i}\right)}{Fr(Fr+1)(Fr-1)} \tag{S6-1}$$

$$\overline{v_z} = \frac{v_{sheet} A_{sheet}}{\pi R_{CNT}^2} \tag{S6-2}$$

where, $Z_{driving,i}$ and $Z_{driven,i}$ are the average Z-coordinate values of driving and driven sheets at i frame, respectively; A_{sheet} is the area of the movable graphene sheets.

Thomas et al.[14] reported a series of water velocities in nanotubes using the similar simulation approaches as in the present work. They used a hydraulic conductivity $\gamma = L_t v / \Delta P$ as a criterion to characterizing water transport in nanotubes with different diameters under external pressure. They obtained the γ valued from 2.23 to 7.71×10^{-15} $m^2/Pa \cdot s$ with CNT radius from 0.42 to 0.83 nm. In our work, the values of γ are 0.90 to 2.99×10^{-15} $m^2/Pa \cdot s$ with CNT radius from 0.35 to 0.63 nm, which is slightly smaller than the values from literature.

Criteria of Hydrogen bond: The hydrogen bond is calculated as follows: all oxygen atoms are traversed to calculate the distance with other oxygen atoms *vide ante*, and we select the pair of water molecules with the distances from 2.5 Å to 4 Å. Since there are four hydrogen atoms in the mentioned water-pair, we consider the hydrogen atom with angle of O-H-O more than 90° as the hydrogen taking part in a hydrogen-bond. After the distance and angle are calculated, we make a 2-dimensional histogram (**Fig. 4c**) with proper subintervals of distance and angle.

To find the properties of hydrogen bond in CNTs, we need to obtain the criteria defining the hydrogen bond. Martí[15, 16] listed three conditions to define a hydrogen bond, briefly, the distance of oxygens (r_{OO}) should be less than 3.6 Å; the distance between acceptor O and donor H (r_{OH}) should be less than 2.4 Å; the angle between the O-O direction and the O-H bond within one molecule (α_O) should be less than 30°. As the acceptor O and donor O-H construct a triangle and length of O-H bond (B_{OH}) is fixed around 96 pm, we use r_{OO} and the angle of O-H-O (α_H) as criteria for convenience. The equation is written as:

$$\begin{cases} r_{OH} = B_{OH} \cos\alpha_H + \sqrt{r_{OO}^2 - B_{OH}^2 \sin^2 \alpha_H} \\ \sin\alpha_O = \dfrac{r_{OH}}{r_{OO}} \sin\alpha_H \end{cases} \tag{S5}$$

the criteria of hydrogen bond are then simplified into the following two conditions approximately: the angle of O-H-O (α_H) is more than 140°; r_{OO} is less than 3.3 Å.

Eigen peaks of confined water transport: Trajectory of 200 ps (20000 frames) for water transport in CNTs with pressure is first obtained following the step described in Part VI. Only water molecules in CNTs are reserved for further analysis. We use IR Spectra Density Calculator with correction of harmonic in VMD 1.9.1 to calculate the amplitude at wave number from 0 to 1000 cm^{-1} (**Fig. S4**). In order to find the peak of the data, we select the maximum value for every 5 cm^{-1} width of wave number and smooth the data with a 5-point moving average method (**Fig. S5a**). After the pretreatment of data, a two-peak Gaussian fitting is performed (**Fig. S5b**).

VIII. The effects of CNT entrance

We extract the data of water distribution along the direction of Z-axis in or adjacent to

CNT from trajectories of equilibrium progress in MD shown in paragraph 2 of SI III. Then, the probability of a single water molecule is obtained as shown in **Fig. S6a**, and the potential barrier for water entrance into different CNT radius is shown in **Fig. S6b**.

IX. Concerned parameters in main body and Supporting Information

A, A_{sheet}: average area of a single carbon on the surface of nanotube, area of the graphene sheets.
a: The distance between the test point and origin.
B_{ij}: bond length of atom i and j.
Fr: frame number of trajectory file.
h: CNT length.
k_0: a fixed constant equaling to KL^2/M while K, L and M are stiffness, length and mass of the "spring" respectively. K^*,L^*, $A^*$and M^* are stiffness, length, area and mass of a single unit of the "spring".
l_{num} and a_{num} are numbers of the units consisting the "spring", *i.e.*, $L=l_{num}{}^*L^*$, $A=a_{num}{}^*A^*$.
m and n: CNT vectors.
L_t: the length of tube.
N, $N(r)$, N_{tot}: number of water molecule or spheres.
N_0: Closest packing number with spheres.
N_A, k and T: Avogadro constant, Boltzmann constant and temperature respectively.
$N_{max,A}$: maximum loop times.
P: pressure of the system, while ΔP is the pressure difference across the nanotube.
Pro: the probability of water molecule in CNT.
R_{CNT}: radius of CNT.
$R_{min,ij}$: the minimum-potential distance of atom i and j, while $R_{min,i}$ and $R_{min,j}$ are defined as $R_{min,ij}=1/2(R_{min,i} + R_{min,j})$
R_s: sphere radius.
r, r_{ij}: distance, distance of atom i and j.
r_{dfp}: distribution function peak of water molecule in CNT.
r_{eff}: effective radius of CNT.
r_{lb}: lower bound of radius variation.
$r(\theta,z)$: distance between the integrate unit and test point.
t_0: time step in simulation.
$U_{LJ}(a)$, U^*_{LJ}, $U(\theta,z)$: total L-J potential at the position with a distance of a from center of CNT, the minimum value of U_{LJ} with the variable a, the contribution of potential at angle of θ and coordination of z.
$u(l,t)$: the displacement of water in CNT at time t and position l.
V_O: overlap volume
Vol: volume.
V_{lb}: lower bound of overlap volume. V_O smaller than V_{lb} will be neglected.

v, $\overline{v}_z$: average velocity of waters in CNT.

x, y and z: axes of the system considered as Cartesian coordinates.

$Z_{driving,i}$ and $Z_{driven,i}$: average Z-coordinate values of driving and driven sheets at i frame respectively.
ε_{ij}: depth of the potential well, while ε_i and ε_j are defined as $\varepsilon_{ij}=(\varepsilon_i\varepsilon_j)^{1/2}$
η: percentage of water molecule numbers comparing with the closest packing number as the function of r.
θ: angular coordinate of inner CNT considered as cylindrical coordinate.
ρ: number density of water molecule.
Φ: the ratio of r_{eff} and R_s.

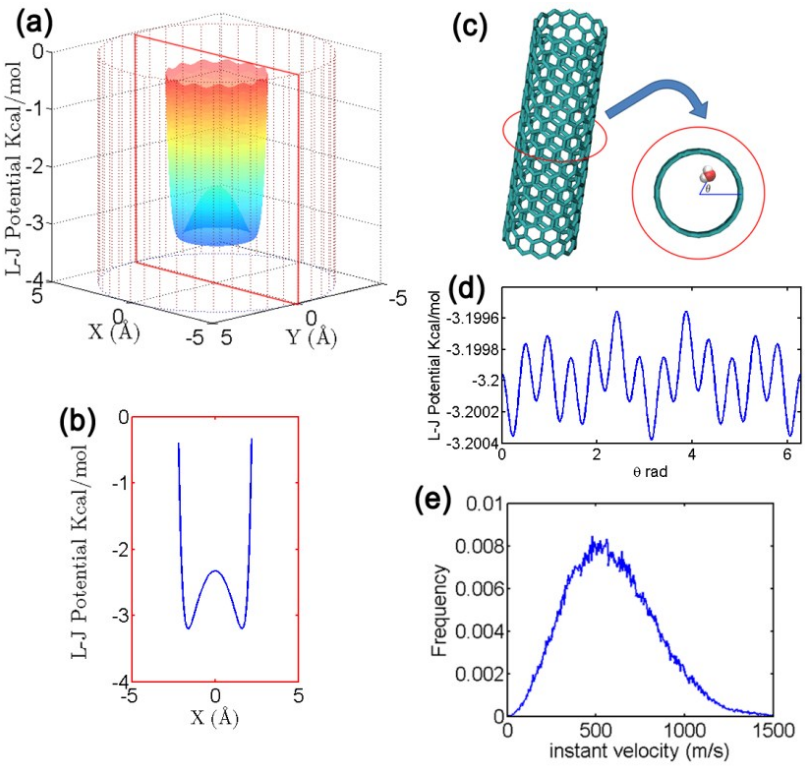

Figure S1. Uniformity of carbon nanotubes. (a) L-J Potential of a single water molecule in CNT (13,0). The dotted cage represents the position of CNT. The potential is calculated with the range of water molecule restrained on surface z=0 and $x^2+y^2 \leq 2.2^2$. (b) The cross-section of (a) at y=0. (c) Schematic of calculating L-J potential fluctuation where red circle shows the plane of z=0. (d) The value of fluctuation for a test water molecule at z=0 and $x^2+y^2=1.85^2$ with variation θ shown in (c), the selected position of water molecule is considered as potential well. (e) Instant velocity distribution of water molecules in CNT at 1.41 GPa and 300 K.

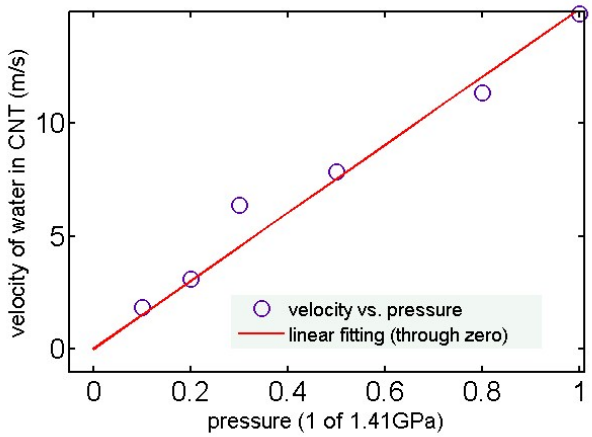

Figure S2. Velocity of water in CNT *v.s.* external pressure.

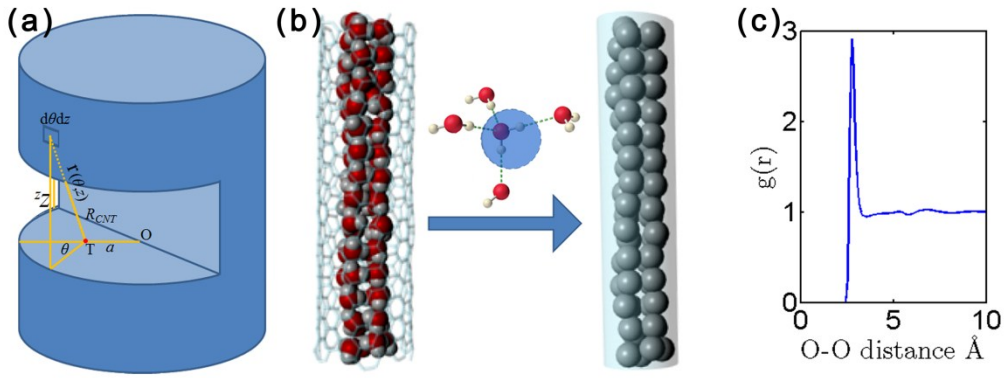

Figure S3. Consider water molecules into spheres. (a) Schematic for calculating L-J interaction between a single water and CNT wall considering CNT as a uniformly cylindrical tube. (b) Schematic of water in CNT and spheres in cylinder. The left figure represents water and CNT wall, while the right one represents corresponding spheres and cylinders. The principle of replacement is obtained between them. (c) Radial pair distribution function of oxygen in water. $g(r)$ is the number density normalized by a homogeneous medium, expressed as $g(r)=N(r)Vol/(4\pi r^2 N_{tot})$, while $N(r)$, Vol and N_{tot} are the numbers, volume and total numbers, respectively.

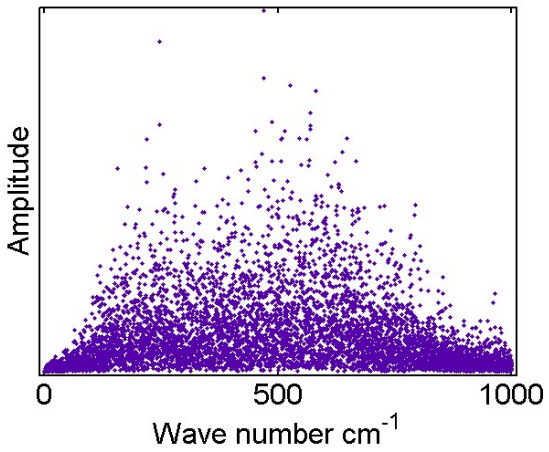

Figure S4. IR spectra of water molecules in an 8-angstrom-length CNT (7,5) extracted from molecule dynamics.

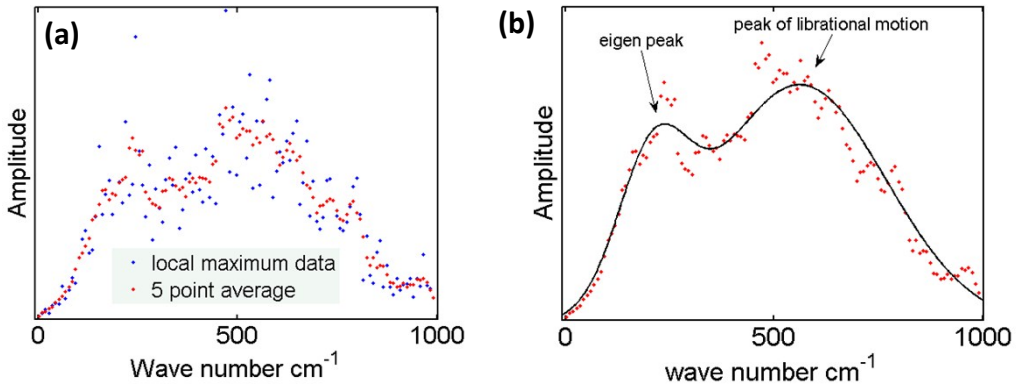

Figure S5. Data extraction from IR spectra of water molecules. (a) local maximum data of every 5 cm^{-1} width of wave number (blue dots) and 5 point average smoothing of the local maximum data (red dots). (b) Two-peak Gaussian fitting of the data from (a).

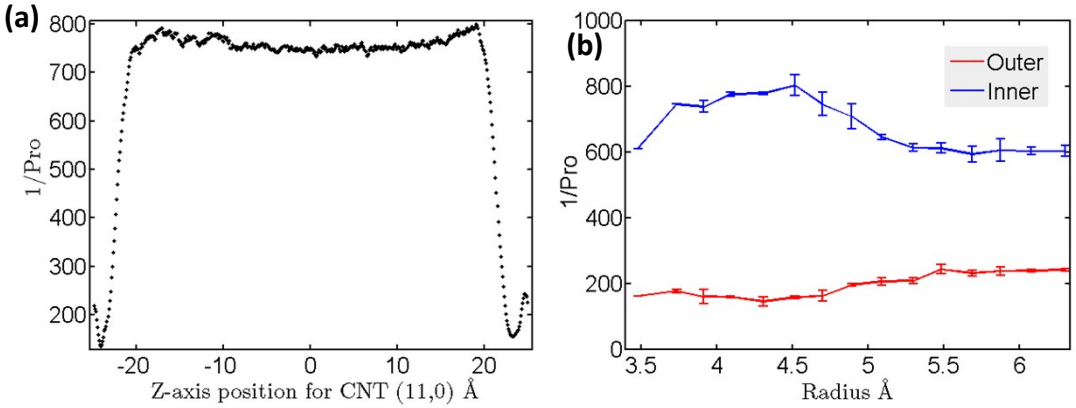

Figure S6. Entrance effect of CNTs. (a) The reciprocal of probability of water molecule in CNT (11,0). The horizontal ordinate refers to the Z-axis of CNT and the entrances locate at ±20 Å. (b) The gap of probability at the entrance of CNTs as function of CNT radius.

Table S1 L-J potential parameters of CNT and TIP3P water.

	ε(kcal/mol)	R_{min}(Å)
CA	-0.070000	1.992400
HT	-0.046000	0.224500
OT	-0.152100	1.768200

Table S2. Comparison of CNTs with the same radius and different chirality.

CNT type	RDF peak position (Å)	water velocity in CNT (m/s)	average Hydrogen bonds per water
(10,6)	2.162	14.30	2.238
(14,0)	2.161	14.97	2.289
ratio	1.0005	1.047	0.9777

Table S3. The detailed data of water molecules distribution in CNT.

CNT type	a_1*	b_1	c_1	a_2	b_2	c_2**
(7,3)	6.722	-123.2	76.22			
(9,1)	1.125	-23.35	17.12	0.199	11.65	39.13
(10,0)	0.4697	-38.39	36.81	0.1326	37.17	35.85
(7,5)	45.03	-168.0	69.38	0.1136	47.69	43.84
(11,0)	0.06427	17.85	60.58	0.08066	83.22	37.54
(9,4)				0.1292	132.3	41.86
(12,0)				0.2192	148.3	25.47
(10,4)				0.2186	165.6	25.60
(13,0)				0.2054	185.5	26.87
(13,1)				0.1916	198.7	29.10
(14,0)				0.1605	213.3	34.30
(14,1)				0.1826	235.5	30.23
(15,0)	239.7	-231.5	82.53	0.1266	247.7	37.74
(15,1)	0.4889	-36.78	47.47	0.07153	279.0	31.52
(15,2)	0.3154	-36.89	56.89	0.06348	295.4	35.00

*The fitting equation is written as: $\rho(r) = a_1 e^{-((r-b_1)/c_1)^2} + a_2 e^{-((r-b_2)/c_2)^2}$

**The parameters b_1, b_2, c_1, c_2 and variable r are with the units of pm. Function ρ and parameters a_1 and a_2 are with the units of $1/Å^3$.

References

1. P. Keblinski, S. K. Nayak, P. Zapol and P. M. Ajayan, *Phys. Rev. Lett.*, 2002, **89**, 255503.
2. J. C. Phillips, R. Braun, W. Wang, J. Gumbart, E. Tajkhorshid, E. Villa, C. Chipot, R. D. Skeel, L. Kale and K. Schulten, *J. Comput. Chem.*, 2005, **26**, 1781-1802.
3. W. Humphrey, A. Dalke and K. Schulten, *J. Mol. Graphics*, 1996, **14**, 33-38.
4. B. R. Brooks, C. L. B. III, A. D. M. Jr, L. Nilsson, R. J. Petrella, B. Roux, Y. Won, G. Archontis, C. Bartels, S. Boresch, A. Caflisch, L. Caves, Q. Cui, A. R. Dinner, M. Feig, S. Fischer, J. Gao, M. Hodoscek, W. Im, K. Kuczera, T. Lazaridis, J. Ma, V. Ovchinnikov, E. Paci, R. W. Pastor, C. B. Post, J. Z. Pu, M. Schaefer, B. Tidor, R. M. Venable, H. L. Woodcock, X. Wu, W. Yang, D. M. York and M. Karplus, *J. Comput. Chem.*, 2009, **30**, 1545-1614.
5. T. Darden, D. York and L. Pedersen, *J. Chem. Phys.*, 1993, **98**, 10089-10092.
6. W. L. Jorgensen, J. Chandrasekhar, J. D. Madura, R. W. Impey and M. L. Klein, *J. Chem. Phys.*, 1983, **79**, 926-935.
7. M. G. Greening, R. Graham and J. Ratz, *Am. Math. Mon.*, 1968, **75**, 192-193.
8. S. Sasloglou, J. Petrou, N. Kanellopoulos and G. Androutsopoulos, *Microporous Mesoporous Mater.*, 2000, **39**, 477-483.
9. R. L. Jernigan and A. Kloczkowski, in *Protein Folding Protocols*, Springer, 2006, pp. 251-276.
10. R. Al-Raoush and M. Alsaleh, *Powder Technol.*, 2007, **176**, 47-55.
11. M. Nishida, M. Okumura and K. Tanaka, *Granular Matter*, 2010, **12**, 337-344.
12. M. R. Garey and D. S. Johnson, *Computer and intractability*, 1979.
13. Y. G. Stoyan and G. Yaskov, *Int. T. Oper. Res.*, 2010, **17**, 51-70.
14. J. A. Thomas and A. J. McGaughey, *Phys. Rev. Lett.*, 2009, **102**, 184502.
15. J. Martı, *J. Chem. Phys.*, 1999, **110**, 6876-6886.
16. M. Gordillo and J. Martı, *Chem. Phys. Lett.*, 2000, **329**, 341-345.